

Forbidden Transitions ($\Delta m = \pm 1$) in the Paramagnetic Resonance Absorption of Mn^{2+} in Calcite†

J. Mankowitz and W. Low

Microwave Division, Department of Physics, The Hebrew University, Jerusalem, Israel

(Received 12 January 1970)

The forbidden transitions of the type $\Delta m = \pm 1$ for Mn^{2+} in single crystals of calcite have been investigated at X-band frequencies. The results can be fitted with the spin Hamiltonian $\mathcal{H} = g\mu_B \vec{H} \cdot \vec{S} + B_2^0 O_2^0 + B_2^2 O_2^2 + B_4^0 O_4^0 + B_4^2 O_4^2 + C_4^3 O_4^3 + A(S_x I_x) + B(S_x I_x + S_y I_y) - g_N \mu_N (\vec{H} \cdot \vec{I}) + Q' [I_z^2 - \frac{1}{3} I(I+1)] + Q'' (I_x^2 - I_y^2)$. At room temperature, the best computer fit for the parameters is

$$\begin{aligned} g_{||} &= 2.0019 \pm 0.0006, & g_{\perp} &= 2.0018 \pm 0.0006, \\ B_2^0 &= 24.99 \pm 0.10, & B_4^0 &= 0.0397 \pm 0.0002, \\ A &= 87.01 \pm 0.04, & B &= 87.26 \pm 0.04, \\ Q' &= 0.174 \pm 0.1, & Q'' \cos 2\phi &= -0.065 \pm 0.1, \end{aligned}$$

$B_4^3 \cos 3\phi - C_4^3 \sin 3\phi = -0.542 \pm 0.04$ (all in units of 10^{-4} cm⁻¹); $g_N \mu_N = (10.11 \pm 2.0) \times 10^{-24}$ erg/G.

I. INTRODUCTION

The paramagnetic resonance spectrum of Mn^{2+} in calcite has been investigated by Mataresse and Kikuchi¹ and the isoelectronic ion Fe^{3+} in calcite by Marshall and Reinberg.² These authors have measured the allowed transitions and have pointed out the importance of the term B_4^3 in the spin Hamiltonian for ion of $S = \frac{5}{2}$. The forbidden transitions, however, have not been previously measured. These transitions involve terms of the quadrupole and nuclear moment of the manganese ions. Since the lines in calcite are very sharp, they lend themselves to evaluation of the total Hamiltonian.

Another aspect of this paper is a comparison of the fit of the parameters obtained from the conventional expansion of the Hamiltonian to the second order of perturbation with the parameters obtained by diagonalization of the full matrix.

II. THEORY

Calcite ($CaCO_3$) has a rhombohedral symmetry. The crystal structure gives rise to two inequivalent calcium sites, each with the point symmetry S_6 . The spin Hamiltonian for Mn^{2+} , substituting for the calcium, is given by

$$V = B_2^0 O_2^0 + B_4^0 O_4^0 + B_4^3 O_4^3 + C_4^3 R_4^3, \quad (1)$$

where B_4^3 and C_4^3 are real and correspond to the real and imaginary parts of B_4^3 as defined by Marshall and Reinberg.² The other inequivalent site has the same spin Hamiltonian, except that one replaces B_4^3 with $-B_4^3$. The operators of O_2^0 and O_4^0 are defined in terms of spherical harmonics by Low,³ Prather,⁴ and Hutchings.⁵ We give only the expressions for O_4^3 and R_4^3 which are not commonly used:

$$\begin{aligned} O_4^3 &= \frac{1}{4} [S_z(S_+^3 + S_-^3) + (S_+^3 + S_-^3)S_z], \\ R_4^3 &= -\frac{1}{4} i [S_z(S_+^3 - S_-^3) + (S_+^3 - S_-^3)S_z]. \end{aligned} \quad (2)$$

The values of these operators in different S manifolds have been tabulated by Low and by Hutchings.

If we include the nuclear part and the effect of the magnetic field, the spin Hamiltonian takes the form

$$\begin{aligned} \mathcal{H} &= g\mu_B \vec{H} \cdot \vec{S} + B_2^0 O_2^0 + B_4^0 O_4^0 + B_4^3 O_4^3 + C_4^3 R_4^3 \\ &+ AS_z I_x + \frac{1}{2} B(S_+ I_- + S_- I_+) - g_N \mu_N \vec{H} \cdot \vec{I} \\ &+ Q' [I_z^2 - \frac{1}{3} I(I+1)] + \frac{1}{2} Q'' [I_x^2 + I_y^2], \\ &S = \frac{5}{2}, \quad I = \frac{5}{2}. \end{aligned} \quad (3)$$

Here A and B determine the hyperfine components and γ the gyromagnetic ratio, and Q' and Q'' the components of the quadrupole tensor in an axial field.

We assume, as indeed this is true in our experiments at a wavelength of 3 cm, that $g\mu_B \vec{H} \cdot \vec{S}$ is larger than any of the other terms of the Hamiltonian. Choosing the axis of quantization along H , which makes an angle of (θ, ϕ) with respect to the crystal axes x, y, z where z is the c axis of the crystal and x and y are the axes in a plane perpendicular, then the Hamiltonian takes the form

$$\begin{aligned} \mathcal{H} &= g\mu_n H S_z - g_N \mu_n H I_x + B_2^0 [\frac{1}{2} (3 \cos^2 \theta - 1) O_2^0 \\ &- 6 \sin \theta \cos \theta O_2^1 + \frac{3}{2} \sin^2 \theta O_2^2] + B_4^0 [\frac{1}{8} (35 \cos^4 \theta \\ &- 30 \cos^2 \theta + 3) O_4^0 - 5 \sin \theta \cos \theta (7 \cos^2 \theta - 3) O_4^1 \\ &+ \frac{5}{2} \sin^2 \theta (7 \cos^2 \theta - 1) O_4^2 - 35 \sin^3 \theta \cos \theta O_4^3 \\ &+ \frac{35}{8} \sin^4 \theta O_4^4] + (B_4^3 \cos 3\phi - C_4^3 \sin 3\phi) \\ &\times [\frac{1}{8} \sin^3 \theta \cos \theta O_4^3 + \frac{1}{4} \sin^2 \theta (4 \cos^2 \theta - 1) O_4^1 \end{aligned}$$

$$\begin{aligned}
& + \frac{1}{2} \sin\theta \cos^3\theta C_4^2 + \frac{1}{4} (4 \cos^4\theta + 3 \cos^2\theta - 3) O_4^3 \\
& - \frac{1}{8} \cos\theta \sin\theta (3 + \cos^2\theta) O_4^4 + (B_4^3 \sin 3\phi + C_4^3 \cos 3\phi) \\
& \times \left[\frac{3}{4} \sin^2\theta \cos\theta R_4^1 + \frac{1}{4} \sin\theta (3 \cos^2\theta - 1) R_4^2 \right. \\
& + \frac{1}{4} \cos\theta (9 \cos^2\theta - 5) R_4^3 - \frac{1}{8} \sin\theta (1 + 3 \cos^2\theta) R_4^4 \\
& + (A \cos^2\theta + B \sin^2\theta) S_z I_z + \frac{1}{4} [A \sin^2\theta + B(1 + \cos^2\theta)] \\
& \times [S_+ I_- + S_- I_+] + \frac{1}{4} (A - B) \sin^2\theta [S_+ I_+ + S_- I_-] \\
& - \frac{1}{2} (A - B) \sin\theta \cos\theta [S_z (I_+ + I_-) + (S_+ + S_-) I_z] \\
& + \left[\frac{1}{2} Q' (3 \cos^2\theta - 1) + \frac{3}{2} Q'' \sin^2\theta \cos^2\phi \right] \\
& \times \left[I_z^2 - \frac{1}{3} I(I+1) \right] . \tag{4}
\end{aligned}$$

The very small nondiagonal part of Q has been neglected in the above transformation.

A second-order perturbation gives the following expressions for the resonance field.

A. Fine Structure

$$\begin{aligned}
H_{\text{FS}} &= H_0 + T + (1/H_0)[\zeta^2 - 5\tau^2 + 190\lambda\zeta - 90\sigma\tau], \\
\Delta M &= \pm \frac{3}{2} \mp \pm \frac{1}{2}, \\
H_{\text{FS}} &= H_0 + (1/H_0)[4\zeta^2 - 8\tau^2 - 120\lambda\zeta + 360\sigma\tau], \\
\Delta M &= + \frac{1}{2} \mp - \frac{1}{2}, \\
T &= [3B_2^0(3 \cos^2\theta - 1) - \frac{75}{2} B_4^0(35 \cos^4\theta - 30 \cos^2\theta + 3) \\
& + \frac{75}{2} \bar{B}_4^3 \sin^3\theta \cos\theta], \\
\bar{B}_4^3 &= B_4^3 \cos 3\phi - C_4^3 \sin 3\phi, \\
H_0 &= \frac{h\nu}{g\mu_B}, \text{ where } \nu = \text{frequency of rf field.} \tag{5}
\end{aligned}$$

$$\zeta = -6B_2^0 \sin\theta \cos\theta,$$

$$\tau = \frac{3}{2} B_2^0 \sin^2\theta,$$

$$\begin{aligned}
\lambda &= -5B_4^0 \sin\theta \cos\theta (7 \cos^2\theta - 3) \\
& + \frac{1}{4} \bar{B}_4^3 \sin^2\theta (4 \cos^2\theta - 1),
\end{aligned}$$

$$\sigma = \frac{5}{2} B_4^0 \sin^2\theta (7 \cos^2\theta - 1) + \frac{1}{2} \bar{B}_4^3 \sin\theta \cos^3\theta.$$

All the constants above are expressed in Gauss, by the conversion $B_2^0/g\mu_B \rightarrow \bar{B}_2^0$, etc.

B. Hyperfine Structure

The hyperfine contribution to the energy of the state $|M, m\rangle$ is given by

$$\begin{aligned}
E_{\text{HFS}} &= (A \cos^2\theta + B \sin^2\theta) Mm - g_n \mu_n Hm \\
& + \left[\frac{1}{2} Q' (3 \cos^2\theta - 1) + \frac{3}{2} Q'' \sin^2\theta \cos 2\phi \right] \\
& \times \left[m^2 - \frac{1}{3} I(I+1) \right] + \frac{B^2}{2gBH_0} \{m[M^2 - S(S+1)] \\
& + M[I(I+1) - m^2]\} + (\text{third and higher orders}). \tag{6}
\end{aligned}$$

The positions of the lines involving a nuclear

TABLE I. Expression for $a_{mm'}$, $b_{mm'}$, $c_{Mmm'}$, as used in first-order Hamiltonian [Eq. (7)].

	$m' = m + 1$	$m' = m - 1$
$a_{mm'}$	$-\frac{gN\mu_N}{g\mu_B}$	$+\frac{gN\mu_N}{g\mu_B}$
$b_{mm'}$	$2m + 1$	$-2m + 1$
$c_{Mmm'}$	$M - m - 1$	$-(M + m - 1)$

flip ($\Delta m = \pm 1$) are given to first order by

$$H(M, m \rightleftharpoons M - 1, m') = H_{\text{FS}} + a_{mm'} H + b_{mm'} Q + c_{Mmm'} K + H_c,$$

$$Q = \frac{1}{2} Q' (3 \cos^2\theta - 1) + \frac{3}{2} Q'' \sin^2\theta \cos 2\phi, \tag{7}$$

$$K = A \cos^2\theta + B \sin^2\theta.$$

H_c is the correction to the field from higher-order perturbing terms. The expressions a , b , and c are given in Table I. The second order correction is

$$\begin{aligned}
H_c^{(2)} &= (B^2/2H_0) \left[-\frac{35}{2} - 2(m+1)(M+1) \right. \\
& + (M-m)(M-m-1) \left. \right], \quad m' = m + 1 \\
& = \frac{B^2}{2H_0} [(m-M)(M+m-1)], \quad m' = m - 1. \tag{8}
\end{aligned}$$

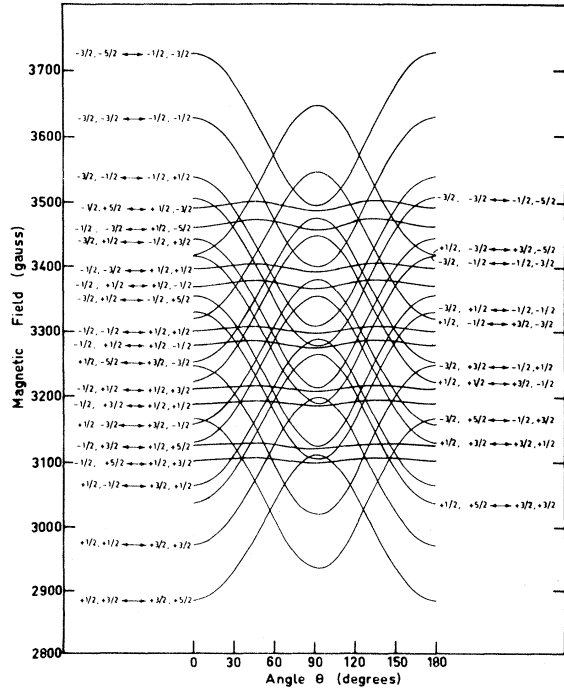


FIG. 1. Angular dependence of the forbidden transition of the Mn^{2+} spectrum in calcite.

TABLE II. $\Delta = H$ (calculated) $- H$ (measured). A comparison of the field values, calculated using second-order perturbation terms and by diagonalizing the complete spin Hamiltonian. $H = H(M, m, M-1, m')$.

M	m	m'	H (measured)	$\theta = 0^\circ$		H (measured)	$\theta = 90^\circ$	
				Perturbation 2nd order	Diag		Perturbation 2nd order	Diag
$\frac{3}{2}$	-	$m-1$	3285.9	-1.3	0.1	3510.3	3.7	4.6
	-	$m-1$	3188.0	-0.8	-0.1	3414.4	2.7	2.0
	+	$m-1$	3093.2	-0.7	-0.6	3320.6	2.2	0.8
	+	$m-1$	2999.4	1.0	0.5	3228.8	2.4	0.7
	+	$m-1$	2908.6	2.2	0.9	3140.1	2.0	0.3
	-	$m+1$	3453.2	2.2	1.5	3686.7	2.5	-3.0
	-	$m+1$	3354.3	0.4	0.0	3582.7	3.7	-0.6
	-	$m+1$	3255.3	0.2	0.5	3482.8	3.5	1.0
	+	$m+1$	3159.5	-0.5	0.8	3388.9	-0.3	-0.4
	+	$m+1$	3064.6	0.4	2.7	3297.1	-3.5	-1.0
	-	$m-1$	3527.6	-0.9	0.7	3522.5	-0.9	0.9
	-	$m-1$	3432.8	-3.4	-2.8	3426.7	-1.9	-0.9
+	$m-1$	3334.9	-0.3	-0.4	3330.8	-0.3	0.1	
+	$m-1$	3244.1	-1.7	-2.4	3240.0	-1.2	-1.4	
+	$m-1$	3154.4	-1.5	-3.0	3150.3	-0.5	-1.5	
$\frac{1}{2}$	-	$m+1$	3497.0	2.2	1.0	3492.9	4.3	0.1
	-	$m+1$	3404.0	-1.5	-1.9	3401.2	-1.5	-2.8
	-	$m+1$	3311.4	-2.7	-2.2	3307.3	-2.6	-1.5
	+	$m+1$	3219.6	-2.2	-1.0	3216.6	-4.2	-1.0
	+	$m+1$	3130.9	-2.2	-0.6	3128.9	-6.3	-1.6
	-	$m-1$	3766.3	0.0	1.4	3530.7	0.0	2.0
	-	$m-1$	3667.3	1.5	2.0	3435.8	-2.0	-0.2
	+	$m-1$	3575.6	-1.5	-1.6	3342.0	-2.5	-0.9
	+	$m-1$	3478.7	3.2	2.6	3245.1	2.8	3.6
	+	$m-1$	3389.9	2.4	1.1	3154.4	4.5	4.1
	-	$m+1$	3542.9	1.7	0.2	3311.4	0.6	-0.7
	-	$m+1$	3452.2	1.1	0.9	3220.7	-1.0	0.6
-	$m+1$	3364.5	0.1	0.7	3135.0	-5.1	-1.6	
+	$m+1$	3279.8	-1.3	-0.4	3048.3	-5.6	-1.2	
+	$m+1$	3196.2	-1.2	-0.5	2962.7	-4.5	-0.4	
		Δ_{rms}		1.7	1.5	Δ_{rms}	3.1	1.8

TABLE III. $\Delta_{rms} = [\frac{1}{30}(H_{calc} - H_{meas})^2]^{1/2}$. Comparison of values obtained using second-order perturbation results, and by numerical diagonalization of the spin Hamiltonian.

θ	Δ_{rms} (Gauss)													
	0°	15°	30°	45°	60°	75°	90°	105°	120°	135°	150°	165°		
2nd order pert	1.7	1.7	2.3	2.4	2.7	2.7	3.1	2.8	2.9	2.7	2.3	1.8		
Diag matrix	1.5	1.5	1.8	1.8	1.7	1.6	1.8	1.5	1.8	1.8	1.9	1.5		

TABLE IV. Spin Hamiltonian parameters obtained from the forbidden transitions of Mn^{2+} in $CaCO_3$.

$g_{ } = 2.0019 \pm 0.006$	$g_{\perp} = 2.0018 \pm 0.0006$
$B_2^0 = 24.99 \pm 0.10$	$B_4^0 = 0.0397 \pm 0.0002$
$A = 87.01 \pm 0.04$	$B = 87.26 \pm 0.04$
$Q' = 0.17 \pm 0.1$	$Q'' \cos 2\Phi = -0.065 \pm 0.1$
$B_2^3 \cos 3\Phi - C_4^3 \sin 3\Phi = -0.542 \pm 0.04$ all in units of 10^{-4}	
$cm^{-1} \gamma\beta_N = (10.11 \pm 2.0) 10^{-24}$ erg/G	

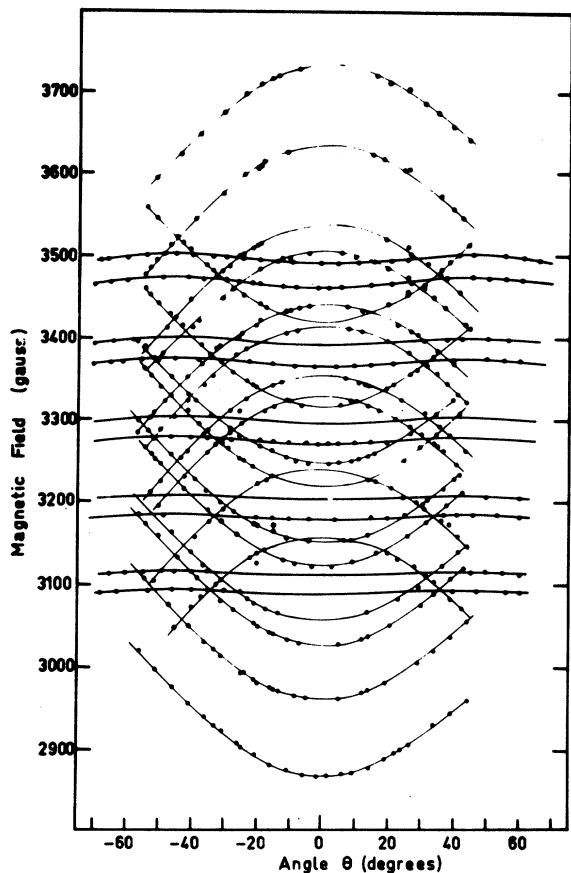


FIG. 2. Angular dependence of the forbidden transition of Mn^{2+} in calcite near $\theta = 0^\circ$ but with a different value of the azimuthal angle.

It is worth while to note that the Hamiltonian contains linear terms in $g_n \mu_n$ and Q , and hence a careful measurement permits the evaluation of these terms.

In most publications, the Hamiltonian is evaluated using the expansion of the spin Hamiltonian to second or higher perturbation. We have compared the values of the parameters obtained using the above approximate Hamiltonian with those parameters obtained by direct diagonalization of the 36×36 matrix.

III. EXPERIMENTAL RESULTS AND DISCUSSION

The crystal was oriented in the following manner. The crystal was cleaved to give a rhombohedron of 2-mm edge. A special crystal holder was constructed so that the c axis was exactly defined with respect to the crystal holder and hence with respect to the resonance cavity. There were two possibilities of mounting the crystal with (i) either c axis in the horizontal or (ii) in the ver-

tical plane and perpendicular to the magnetic field. In the first orientation, ϕ is fixed and θ is varied, or the magnetic field direction is changed. In the second case, $\theta = 90^\circ$ and one measures the changes of the spectrum with respect to ϕ .

Figure 1 shows the angular dependence of the spectrum of one of the two inequivalent sites. In principle, the values of H at $\theta = 0^\circ$ and 90° are sufficient to establish all parameters except B_4^3 and C_4^3 . These two may be obtained as the linear combination $B_4^3 \cos 3\phi - C_4^3 \sin 3\phi$ from intermediate angles. Figure 2 shows the spectrum about $\theta = 0^\circ$, but with a different azimuthal angle ϕ . It is clearly seen that the spectrum is not symmetrical about $\theta = 0^\circ$ because of the change of $\phi \rightarrow \pi + \phi$ as θ goes through zero.

In Table II, we present the measured values of the various transitions, the calculated position using second-order perturbation theory, and the calculated position by direct diagonalization of the complete spin Hamiltonian. The results are given both for $\theta = 0^\circ$ and 90° . Similar results are obtained for $\theta = 0^\circ$ and 180° .

The root mean square deviation is given both for the perturbation theory and direct diagonalization. In Table III are listed the rms deviations for different angles of θ from 0° to 165° .

Comparison of the data using these two methods shows that there is a better fit at all angles using the direct diagonalization of the total matrix.

We have also measured the forbidden transitions corresponding to $\Delta M = \pm \frac{3}{2} \mp \pm \frac{3}{2}$ at angles close to $\theta = 0^\circ$ and 180° and between 10° and 40° . However, at other orientations, the lines could not be followed because of the lower intensity and in the main because of the over-lap with the stronger allowed transitions. The measured values are not included in Tables. They do not change the obtained values of the different parameters.

The values of the parameters obtained are given in Table IV.

These results are in agreement with those found earlier by Hurd *et al.*,⁶ although there is a slight deviation in the value of A which is outside the combined error.

Evaluation of the nuclear moments and the quadrupole moment depends on the knowledge of the $\langle 1/r^3 \rangle$ and the gradient in the crystal.

The value of γB_n found by us is somewhat larger than that obtained by NMR methods.

ACKNOWLEDGMENTS

The authors gratefully acknowledge the assistance of and discussions with J. Bronstein-Shaham and S. Maniv.

[†]Acknowledgment is made to the donors of The Petroleum Research Fund, administered by the American Chemical Society, for partial support of this research.

¹L. M. Mataresse and C. Kikuchi, *J. Chem. Phys.* **33**, 601 (1960); see also L. M. Mataresse, *J. Chem. Phys.* **34**, 336 (1961), who has also observed some of the forbidden transitions.

²S. A. Marshall and A. R. Reinberg, *Phys. Rev.* **132**, 134 (1963).

³W. Low, in *Solid State Physics*, Suppl. 2, edited by

F. Seitz and D. Turnbull (Academic, New York, 1960).

⁴J. L. Prather, *Atomic Energy Levels in Crystals*, Natl. Bur. Std. Monograph No. 19 (U. S. Government Printing Office, Washington, D. C., 1961).

⁵M. T. Hutchings, in *Solid State Physics*, edited by F. Seitz and D. Turnbull (Academic, New York, 1964), Chap. XVI.

⁶F. R. Hurd, M. Sachs, and W. O. Hershberger, *Phys. Rev.* **93**, 373 (1954).

Jahn-Teller Distortions of Ag^{2+} Ions in SrF_2 and CaF_2 by Odd Modes

R. C. Fedder

Department of Physics, University of Cincinnati, Cincinnati, Ohio 45221

(Received 14 August 1969; revised manuscript received 3 February 1970)

An anisotropic EPR spectrum of Ag^{2+} ions has been observed at 4.2°K in single crystals of CaF_2 and SrF_2 that have been doped with silver. X rays convert the silver from the Ag^{1+} to the Ag^{2+} state. The results may be fitted with spin Hamiltonians with $S = \frac{1}{2}$, $g_{\parallel} = 1.997 \pm 0.001$ and $g_{\perp} = 2.106 \pm 0.001$ for CaF_2 , and $g_{\parallel} = 1.988 \pm 0.001$ and $g_{\perp} = 2.130 \pm 0.001$ for SrF_2 . Hyperfine interactions with the silver nucleus are not resolved, but are expected to be small from symmetry considerations. Hyperfine interactions with two equivalent fluorines are observed and have the characteristic 1:2:1 intensity ratio with $A_{\parallel} = 58.6 \times 10^{-4} \text{ cm}^{-1}$ and $A_{\perp} = 14.5 \times 10^{-4} \text{ cm}^{-1}$ for $\text{CaF}_2:\text{Ag}^{2+}$, and $A_{\parallel} = 30.6 \times 10^{-4} \text{ cm}^{-1}$ and $A_{\perp} = 14.6 \times 10^{-4} \text{ cm}^{-1}$ for $\text{SrF}_2:\text{Ag}^{2+}$. Additional hyperfine structure from four other fluorine nuclei can be resolved when the magnetic field is along a $\langle 110 \rangle$ direction. Optical absorption bands are observed in the x-rayed $\text{CaF}_2:\text{Ag}^{2+}$ at 25 550 and 19 000 cm^{-1} . One of the optical absorption bands and the g shift can be correlated by assuming that the Ag^{2+} excited state mixes with the fluorine ligands. This physical system is unusual in that the silver ions distort from cubic symmetry by moving off center in $\langle 110 \rangle$ directions away from the central position and should have an electric dipole moment. In the distorted position, the hole in the d shell of Ag^{2+} is shared with a pair of $\langle 100 \rangle$ -oriented fluorine ions.

I. INTRODUCTION

Jahn-Teller effects¹ have been a subject of increasing attention recently. A considerable amount of theoretical effort has gone into the study of static and dynamic Jahn-Teller effects for the doublet (Γ_3^-) ground state. Bersuker,² Ham,³ and O'Brien⁴ have made important contributions beyond the earlier work of Opik, Pryce, and others.⁵ Coffman⁶ and Höchli⁷ have recently found some experimental evidence for tunneling effects in the electron-paramagnetic-resonance (EPR) spectrum of Cu^{2+} in MgO and Sc^{2+} in CaF_2 and SrF_2 .

Far less information is available on the distortions of triplet ground states, and the theory appears to be more complicated and less developed. Ham³ has developed a theory of dynamical quenching of the orbital angular momentum to successfully explain the reduced g shifts of some para-

magnetic ions that have triplet ground states.

Both Ham⁸ and Sturge⁹ have recently reviewed the experimental and theoretical status of Jahn-Teller effects.

Relatively few examples of static Jahn-Teller effects have been observed for triplet states. One example is the work of Estle *et al.*¹⁰ and Morigaki¹¹ who have attributed an anisotropic spectrum of Cr^{2+} to distortions along a line bisecting the angle to a nearest-neighbor pair of sulphurs in CdS . Similar spectra have been observed for Cr^{2+} in ZnSe , CaF_2 , and CdF_2 . A model related to the one presented in this paper may apply to the above-mentioned experiments. Recently, Ham⁸ has reviewed the experimental situation for Jahn-Teller effects in orbital triplet states.

In this article, we will present results for the static distortions of the Ag^{2+} ion in CaF_2 and SrF_2 ,¹² where the ground electronic state is a Γ_5^- triplet